Fluorescence Intensity and Lifetime Distribution Analysis: Toward Higher Accuracy in Fluorescence Fluctuation Spectroscopy

Kaupo Palo,* Leif Brand,* Christian Eggeling,* Stefan Jäger,* Peet Kask,*† and Karsten Gall*
*Evotec OAI, D-22525, Hamburg, Germany and †Institute of Experimental Biology, Harku 76902, Estonia

ABSTRACT Fluorescence fluctuation methods such as fluorescence correlation spectroscopy and fluorescence intensity distribution analysis (FIDA) have proven to be versatile tools for studying molecular interactions with single molecule sensitivity. Another well-known fluorescence technique is the measurement of the fluorescence lifetime. Here, we introduce a method that combines the benefits of both FIDA and fluorescence lifetime analysis. It is based on fitting the two-dimensional histogram of the number of photons detected in counting time intervals of given width and the sum of excitation to detection delay times of these photons. Referred to as fluorescence intensity and lifetime distribution analysis (FILDA), the technique distinguishes fluorescence species on the basis of both their specific molecular brightness and the lifetime of the excited state and is also able to determine absolute fluorophore concentrations. The combined information yielded by FILDA results in significantly increased accuracy compared to that of FIDA or fluorescence lifetime analysis alone. In this paper, the theory of FILDA is elaborated and applied to both simulated and experimental data. The outstanding power of this technique in resolving different species is shown by quantifying the binding of calmodulin to a peptide ligand, thus indicating the potential for application of FILDA to similar problems in the life sciences.

INTRODUCTION

Fluorescence-based measurements offer unprecedented sensitivity and flexibility for a variety of scientific and industrial applications. These factors, combined with new developments in instrumentation, data analysis, fluorescent probes, and applications have contributed to the rapid growth in this field over recent decades. Such an explosive increase in popularity would barely have been imagined 150 years ago when the fluorescence phenomenon was first observed (Stokes, 1852).

As modern fluorescence microscopy has made the observation of single molecules possible, a powerful set of applications has emerged that yield detailed information about complex molecules and their reaction pathways (Keller et al., 1996; Xie and Trautman, 1998). One of the most commonly cited fluorescence techniques with single-molecule sensitivity is fluorescence correlation spectroscopy (FCS) which can resolve different species on the basis of different translational diffusion coefficients (Magde et al., 1972; Elson and Magde, 1974; Rigler et al., 1993). Recently, this fluorescence fluctuation method found its counterpart in fluorescence intensity distribution analysis (FIDA), a technique that discriminates different fluorescent species according to their specific molecular brightness (Kask et al., 1999; Chen et al., 1999). Both FCS and FIDA have also been extended to variants with two detectors monitoring different polarization components or emission bands of fluorescence; fluorescence cross-correlation (Kask et al., 1989; Schwille et al., 1997) and two-dimensional (2D)-FIDA (Kask et al., 2000). 2D-FIDA is worthy of particular mention due to its impressive statistical accuracy. The superior quality of data associated with 2D-FIDA has made it a method of choice for a number of high throughput drug-screening applications (Ullmann et al., 1999).

A very promising feature of FIDA is its ability to be combined with other fluorescence (fluctuation) methods, such as FCS. The recently published fluorescence intensity multiple distributions analysis (FIMDA) technique allows the simultaneous determination of diffusion coefficients and specific brightness values from a single measurement (Palo et al., 2000). In this paper, we introduce a method that combines FIDA with fluorescence lifetime analysis (FLA), which we refer to as fluorescence intensity and lifetime distribution analysis (FILDA).

Many applications make use of the fluorescence lifetime as an intrinsic molecular property that is sensitive to any changes of the molecule's direct environment (Lakowicz, 1983). However, in contrast to fluctuation methods mentioned above, FLA is essentially a macroscopic technique. Fluorescence decay times can therefore be measured without the constraints imposed by fluorescence fluctuation measurements (i.e., confocal detection volume, low fluorophore concentration, etc.). In fact, conventional FLA measurements ignore signal fluctuations because they integrate over the whole signal. Two main methods are generally applied for FLA; frequency-domain and time-domain data acquisition. FLA applied in the frequency domain uses sinusoidally modulated light to calculate the fluorescence lifetime from the shift and demodulation of the fluorescence emission (Weber, 1981; Clegg and Schneider, 1996). In the time domain, the fluorescence lifetime is determined from the time-dependent decay of the fluorescence emission after a brief excitation pulse. The most common set-up in this case is that of time-correlated single-photon counting

Submitted May 7, 2001, and accepted for publication April 19, 2002.

Address reprint requests to Karsten Gall, Evotec OAI, Schnackenburgallee 114, D-22525 Hamburg, Germany. Tel.: +49-40-560-81-295; Fax: +49-40-560-81-222; E-mail: Karsten.Gall@evotecoai.com.

0006-3495/02/08/605/14 $2.00

(TCSPC), which directly observes the excitation-to-detection delay times of each individual photon that is detected (Wild et al., 1977; O'Connor and Phillips, 1984). The experimentally collected excitation-to-detection delay time histogram contains contributions from all the fluorescent species present in the sample that may be distinguished by their individual fluorescence lifetimes. It is worth noting that, unlike FIDA, FLA is not able to directly resolve absolute concentrations and specific brightness values, but gives only fractional count rates. However, if a linear relation between fluorescence intensity and lifetime may be assumed, which is the case when there is only dynamic quenching, concentrations of different species can be estimated. In a number of applications, FLA is applied at extremely low concentrations, where fluorescence photons are only detected when a single particle happens to diffuse through the detection volume and hence gives rise to a fluorescence burst. By analyzing only the photons arising from such a single burst, the direct identification of single molecules via their fluorescence lifetime can be realized (Zander et al., 1996; Keller et al., 1996; Muller et al., 1996; Brand et al., 1997). This single-molecule technique has been optimized by burst integrated fluorescence lifetime (BIFL) (Keller et al., 1996; Fries et al., 1998; Eggeling et al., 2001). To handle delay time histograms of low photon numbers within a single burst, statistical methods have been applied that are based on the concept of the maximum-likelihood estimator (Bajzer et al., 1991; Köllner and Wolfrum, 1992; Zander et al., 1996; Brand et al., 1997; Enderlein et al., 1997; Maus et al., 2001). Improvement in the accuracy of the identification and quantification of single molecules has been achieved through the simultaneous determination of additional fluorescence parameters such as intensity, intensity ratio, polarization, etc. (Bunfield and Davis, 1998; Prummer et al., 2000; Eggeling et al., 2001). Using these additional parameters, multidimensional histograms may be generated (van Orden et al., 1998; Herten et al., 2000; Eggeling et al., 2001). However, a full mathematical description of these multidimensional histograms is still missing, and analysis has therefore been limited to the use of center-of-gravity techniques.

In FIDA experiments, photon-count numbers are recorded in consecutive counting time intervals (Kask et al., 1999). The extension of FIDA to a polarization or wavelength-sensitive set-up has also been demonstrated (Kask et al., 2000). In both cases, a full theory has been developed that permits prompt and accurate fitting of theoretical distributions against the corresponding histogram. The versatility of the FIDA theory also enables its combination with FLA, constituting FILDA. Using FILDA, it is possible to discriminate fluorescent species according to both their fluorescence lifetime and their specific brightness. Additionally, it is possible to determine mean particle numbers (absolute concentrations) of the species present, a parameter that is not that directly accessible using conventional FLA.

In contrast to single molecule techniques, such as BIFL, that search for fluorescence bursts from single molecules above a certain threshold intensity, FILDA analyses the relative fluctuations of the whole data stream and thus accounts for the possibility of simultaneous photon emission from different molecules. Therefore, FILDA can be applied at significantly higher concentrations than BIFL and leads to a tremendous reduction in the necessary data acquisition time, with acquisition times as short as one second being possible.

In this paper, we will elaborate in detail the theory behind FILDA. Its applicability and its statistical accuracy will be shown by analyzing data from a dye mixture and comparing the results with those from FLA and FIDA. Simulations based on a random walk algorithm allow an accurate prediction of the statistical errors associated with each of these methods, which will then be used to reveal their dependency on the dye concentration. The attractiveness of FILDA will further be demonstrated by monitoring the binding of calmodulin to a peptide ligand, confirming a broad applicability in the life sciences.

THEORY

As described in detail elsewhere (Kask et al., 1999), the central task of FIDA is fitting a theoretical photon count number distribution, $P^{FIDA}(n)$, against an experimentally collected histogram of photon counts, n, detected in consecutive counting time intervals of a given width, T (e.g., 100 μs). This analysis yields the specific molecular brightness, q, and the absolute concentration, c, for the different species of a sample. The absolute concentration and the specific brightness are parameters known not only in FIDA but also in other fluctuation methods such as FCS. The specific brightness is the mean fluorescence count rate per particle, i.e., the mean detected fluorescence count rate emitted during the transit of a single fluorescent particle through the detection volume. The absolute concentration represents the mean number of fluorescent particles present in the measurement volume at a time.

In the case of time-domain FLA, another histogram is subject to fitting; the excitation-to-detection delay time histogram of single photons, revealing individual fluorescence lifetimes. Usually, a model is selected, describing how different species contribute to a particular theoretical distribution, $P^{FLA}(t)$. According to the most simple model, each species is accounted for by a mono-exponential decay function that is convoluted with the respective instrument response function (IRF). The IRF represents the time profile of the laser excitation pulse as recorded by the detector. Such an analysis allows the division of the overall fluorescence signal into contributions from different constituents of the sample, each characterized by the lifetime, τ, and the

fractional count rate, λ, of the according species. (A species might not necessarily denote different molecules but also different conformational states of the same molecule). In terms of FIDA parameters, the fractional count rate is equivalent to the product of the mean particle number and the specific brightness, $\lambda = cq$.

The function that is experimentally collected and analyzed in FILDA is the histogram, $P(n, \theta)$, of the two jointly determined variables, n and θ. As before, n denotes the number of photon counts detected in the counting time windows, and θ denotes the sum of excitation-to-detection delay times over these n photons. Because the excitation-to-detection times registered by TCSPC are measured in time bins of a certain width (e.g., 0.131 ns), θ actually represents the sum of excitation-to-detection delay-time bin numbers. The main step in FILDA involves the fitting of a theoretical model to the experimentally acquired FILDA distribution, $P(n, \theta)$. For each different fluorescent species of a sample, the fit yields an absolute concentration, c, a specific molecular fluorescence brightness, q, and a fluorescence lifetime, τ. Thus, with FILDA, it is possible to discriminate and quantify different species of a sample through direct determination of an extended number of specific fluorescence parameters, namely q and τ.

The following section outlines how FIDA and FLA are combined into the framework of a comprehensive FILDA theory. A review of the necessary parts of FIDA and FLA is given, and important assumptions are specified. In particular, the reason for selecting the integrated delay time, θ, instead of, e.g., the delay time of each individual detection event, is explained, just as the fundamentals of the representation of generating functions are repeated, which significantly simplify the calculation of theoretical distributions in all FIDA-based methods. Furthermore, possible fitting algorithms are discussed, and the weighting procedure for the least squares method is explained.

Assumptions

Most of the following assumptions used in FILDA have frequently been used in other fluorescence fluctuation methods.

1. Contributions to fluorescence from different species are assumed to be independent.
2. The duration of the photon-counting interval, T, is assumed to be short compared to the typical diffusion time of the fluorescent particles through the detection volume.
3. The light intensity emitted by a particle at a certain position, $\mathbf{r}$, of the observation volume is expressed as a product of its specific brightness, q (mean count rate per particle), and the spatial brightness function, $B(\mathbf{r})$, only.
4. Each fluorescent species has a single characteristic excitation-to-detection delay-time distribution, which is independent of the delay time recorded for the previously detected photon.

Due to assumption 1, contributions from different particles, species, or volume elements to the overall distribution can be combined through convolutions. However, direct calculation of convolutions is a mathematically clumsy and time-consuming process, a problem that is circumvented (as described in detail below) through the use of generating functions (Kask et al., 1999). In this way, the theoretical problem can be reduced to that of a single species.

According to assumption 2 changes in the fluorescence emission during a counting time interval can be neglected and are introduced here only for the sake of simplicity. The movement of particles during a counting time interval slightly decreases the apparent count rate per particle and increases the apparent concentration from their true values—an effect that scales with the width of the time window used and which has been qualified by the theory and practice of FIMDA (Palo et al., 2000). Nevertheless, if one is aware of this shift, one may also apply a relatively long counting time interval.

Also, assumption 3 has a simplifying character rather than being of an absolute necessity. In principle, it neglects other effects such as saturation, triplet transition, and rotational motion.

Assumption 4 is specific for FILDA, necessary for combining any version of FIDA with any version of FLA in the given way. It means that, whenever a particle is excited, it does not remember how much time it has spent in the excited state after the previous excitation. This assumption does not necessarily mean that the delay time distribution of a species must be a mono-exponential function. Rather, FILDA provides a means to distinguish between interpretations of components in the delay time distribution that are indistinguishable by FLA. For example, if a fluorescent molecule undergoes slow transitions between two conformational states of different lifetimes, then, in the context of the present FILDA theory, this molecule consists of two species. If however the nonexponential function is reproduced within each time window (e.g., fast transitions between conformational states compared to the width of the time window), then the species are recognized as a single one by FILDA.

The representation of generating functions

As mentioned previously, the central mathematical task in all FIDA-based theories is the calculation of a theoretical count number distribution that must take into account all contributions from each independent source in the observation volume. According to the assumptions given above, the individual distributions corresponding to each independent source may be combined, albeit in a mathematically inefficient fashion, using convolutions. A much more efficient approach is offered, however, by the theory of generating functions, which has been used in FIDA and FIDA-based theories (Kask et al., 1999, 2000; Palo et al., 2000).

Generating functions are a convenient mathematical representation that is widely used in addressing problems in mathematical statistics. It has the drawback of lacking a simply understandable physical meaning, but, conversely, has the advantage of enabling the formulation of theories that would otherwise be prohibitively complex.

Generally, a generating function, $G(\xi)$, of a distribution, $P(n)$, is defined as

$$G(\xi) = \sum_{n=0}^{\infty} P(n)\xi^n, \tag{1}$$

where ξ is a complex argument. It is, of course, important that the probabilities can be recovered from $G(\xi)$. This can be achieved by making the substitution $\xi \rightarrow \exp(i\phi)$ (i.e., effectively restricting ξ to a complex unit circle) and reinterpreting Eq. 1 as a Fourier series. The generating function is then expressed as

$$G(\phi) = \sum_{n=0}^{\infty} P(n)e^{in\phi}, \tag{2}$$

and the probabilities can be retrieved via the inverse Fourier transform

$$P(n) = \frac{1}{2\pi}\oint G(\phi)e^{-in\phi}\,d\phi. \tag{3}$$

This is particularly convenient for computational purposes, due to the existence of fast Fourier transform algorithms (Brigham, 1974). The 2D generalization of Eq. 1 is straightforward,

$$G(\xi, \eta) = \sum_{n=0}^{\infty}\sum_{\theta=0}^{\infty} P(n, \theta)\xi^n\eta^\theta, \tag{4}$$

where ξ and η are related to the respective Fourier transform parameters, $\xi = \exp(i\phi)$ and $\eta = \exp(i\varphi)$.

The most useful property of generating functions for our purposes is that they are able to map a convolution into a product. Consider the case of two distributions, $P^{(a)}(n)$ and $P^{(b)}(n)$, their convolution, $P^{(ab)}(n)$, is defined as

$$\begin{aligned} P^{(ab)}(n) &= (P^{(a)} \otimes P^{(b)})(n) \\ &= \sum_{k=0}^{n} P^{(b)}(k)P^{(b)}(n-k). \end{aligned} \tag{5}$$

For example, if $P^{(a)}(n)$ is the probability of collecting n photons from source a, and $P^{(b)}(n)$ the probability of collecting n photons from source b, then $P^{(ab)}(n)$ is the probability of collecting the total of n photons from both sources combined. Using the representation of generating functions, this operation is greatly simplified. It can be verified that

$$G^{(ab)}(\xi) = G^{(a)}(\xi)G^{(b)}(\xi). \tag{6}$$

The same relationship holds for the 2D case with $\xi \rightarrow (\xi, \eta)$.

The second key property of generating functions is their linearity. Considering an array of conditional probabilities $P(0|\alpha)$, $P(1|\alpha)$, . . . where α is an additional variable that the probabilities depend on, the unconditional probabilities may be expressed through $P(\alpha)$ as

$$P(n) = \sum_{\alpha} P(\alpha)P(n|\alpha). \tag{7}$$

A similar formula holds in the generating functions case,

$$G(\xi) = \sum_{\alpha} P(\alpha)G(\xi|\alpha). \tag{8}$$

FIDA

The central task in the evaluation of FIDA data is the fitting of a theoretical count number distribution, $P^{FIDA}(n)$, to the measured histogram of photon count numbers. Furthermore, using the first assumption together with the representation of generating functions, the theoretical model can at first be reduced to that of single species. The issue of how the count number distribution, $P^{FIDA}(n)$, is calculated has been addressed by the theory of FIDA (Kask et al., 1999). Therefore, we simply recall here the expression of the generating function of $P^{FIDA}(n)$ for the case of a single species,

$$G(\xi) = \exp\left[c\int (e^{(\xi-1)qTB(\mathbf{r})} - 1)\,dV\right], \tag{9}$$

where $B(\mathbf{r})$ is the spatial brightness function, q is the specific brightness, T is the width of the counting time interval, c is the concentration or more exact the mean number of particles in the confocal volume, and dV is a volume element. The integral on the right side of Eq. 9 can be calculated numerically. The relationship between the spatial brightness and the corresponding volume elements is expressed by an empirical formula of three adjustment parameters, a_1, a_2, and a_3,

$$\frac{dV}{du} = A_0(1 + a_1u + a_2u^2)u^{a_3}, \tag{10}$$

where $u = \ln[B(0)/B(\mathbf{r})]$ and A_0 is a coefficient used to select the unit of volume. Compared to similar earlier published expressions (Kask et al., 1999, 2000; Palo et al., 2000), Eq. 10 has an additional parameter, a_3, that further adds flexibility to describe the actual spatial brightness profile.

FLA

The FILDA approach presented here is based on time-domain FLA. Therefore, two main experimental features have to be taken into account. First, a pulsed laser source, ideally with a pulse duration significantly shorter than the expected fluorescence lifetime, is used to excite the sample.

Second, for every photon that is detected, the excitation-to-detection delay time, t, has to be recorded. Usually these delay times are recorded as bin numbers, k (i.e., each bin corresponds to a certain interval of excitation-to-detection delay times, e.g., (t_k, t_{k+1})), and form a discrete array over the pulse period, T_{pulse}, characterized by a given bin width (i.e., resolution time), Δ. Furthermore, it is necessary to determine the instrument response function (IRF), which is the time profile of the laser excitation pulse as recorded by the detection electronics.

In standard FLA, the histogram of the bin numbers, k, (of all detected fluorescence photons) are fitted to a corresponding theoretical distribution, $P^{FLA}(k)$, from which the fluorescence lifetime values may be retrieved. The expected distribution of delay bin numbers, $P^{FLA}(k)$, is related to the photon-detection function, $P^{FLA}(t)$, which, in turn, is the convolution of the experimentally recorded IRF, P^{FLA}_{IRF}, with a theoretical fluorescence decay function, $P^{FLA}_{decay}(t)$.

$$P^{FLA}(t) = (P^{FLA}_{IRF} \otimes P^{FLA}_{decay})(t). \quad (11)$$

Because a periodical pulsed excitation is applied, we are justified to limit the calculations to a single period $(0, T_{pulse})$ at cyclic boundary conditions. In the most simple case, the decay function is mono-exponential, with a fluorescence lifetime, τ. Due to the limited pulse period, T_{pulse}, contributions from previous excitation pulses have to be taken into account, and the decay function reads as follows,

$$P^{FLA}_{decay}(t) = \frac{1}{\tau}\frac{1}{1 - e^{-T_{pulse}/\tau}} e^{-t/\tau}. \quad (12)$$

Throughout this paper, we assume a mono-exponential decay function for each fluorescent species, thus characterizing each by its (mean) fluorescence lifetime. However, in general, any decay function (e.g., multi-exponential) can be assigned to each species in FILDA without the need of modifying the basic concept of the theory.

At this point, it is worth noting that the argument, t, in Eqs. 11 and 12 denotes real time rather than the bin number, k. To keep the accuracy of the convolution, we have to map both time axes. Therefore, we artificially reduce the bin width, Δ, to 0.02 ns by interpolating the original IRF. After numerically calculating the convolution of Eq. 11, we then revert back to the experimental, cruder time bin axis, k,

$$P^{FLA}(k) = \int_{t_k}^{t_{k+1}} P^{FLA}(t)\, dt. \quad (13)$$

The generating function of $P^{FLA}(k)$ is given by

$$G^{FLA}(\eta) = \sum_k P^{FLA}(k)\eta^k. \quad (14)$$

Here, we note that fluorescence lifetime is not affected by variations in the excitation or detection efficiency, i.e., it is independent of the spatial brightness profile. Thus, $P^{FLA}(k)$ depends only on a single parameter, the fluorescence lifetime, τ.

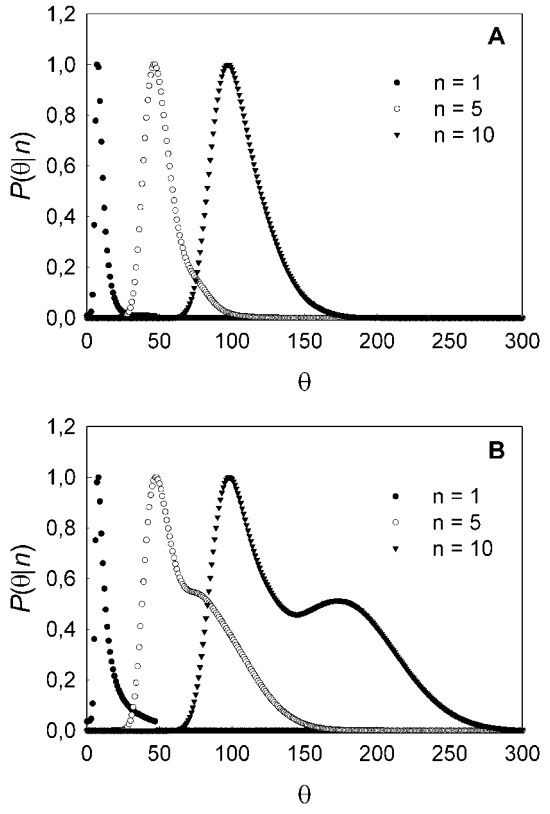

FIGURE 1 Theoretical distributions of the integrated excitation-to-detection delay time bin numbers, $P(\theta|n)$, for different photon count numbers, $n = 1$, 5, and 10. The data have been calculated for two samples, (A) single species and lifetime of 1 ns and (B) a mixture of two species with lifetimes of 1 and 4 ns and equal fractional fluorescence count rates. The case of $n = 1$ corresponds to the case of the ordinary FLA distribution, $P^{FLA}(k)$, of single delay time numbers, k.

The integrated delay time θ

As mentioned before, FIDA collects the number of photon counts, n, within a counting time interval, T. A successful combination of FLA with FIDA can be achieved by constraining FLA to this time window, T. For histogramming, one may now use either each individual delay bin number or the sum of excitation-to-detection delay time bin numbers, θ, of all n photons detected during the time window, T. As illustrated in Fig. 1, the presence of two species can be resolved much easier from the integrated ($n = 5$ and $n = 10$) than from the single photon ($n = 1$) delay time bin distribution. Therefore, we selected the sum of excitation-to-detection delay time bin number, θ, as the specific random variable in FILDA.

With a common time basis, we may now calculate the conditional probability, $P(\theta|n)$, i.e., the probability to detect a certain sum of delay time bin numbers provided there

were n photons detected during the time window, T. According to assumption 1, we may confine ourselves to the case of single species each of which determine $P^{FLA}(k)$ and hence $P(\theta|n)$. Due to assumptions 3 and 4, $P^{FLA}(k)$ neither depends on the number of photons emitted or detected previously, nor on their delay time bin numbers, nor on the coordinates of the molecule emitting the photon. Therefore, $P(\theta|n)$ can be calculated from $P^{FLA}(k)$ by an n-fold convolution, or alternatively, using the generating function representation, from the nth power of the generating function, $G^{FLA}(\eta)$, of $P^{FLA}(k)$,

$$P(\theta|n) = (P^{FLA} \otimes \cdots(n \text{ times})\cdots \otimes P^{FLA})(\theta),$$

$$G(\eta|n) = \sum_{\theta} P(\theta|n)\eta^{\theta} = [G^{FLA}(\eta)]^{n}. \quad (15)$$

Calculation of theoretical FILDA distributions

To find a closed expression for the theoretical model function, $P(n, \theta)$, that can be fitted against the experimentally collected FILDA histogram, we continue studying single species and express $P(n, \theta)$ as a product of two factors, $P^{FIDA}(n)$ and $P(\theta|n)$,

$$P(n, \theta) = P^{FIDA}(n)P(\theta|n). \quad (16)$$

Whereas $P^{FIDA}(n)$ is the FIDA distribution (inverse Fourier transform of Eq. 9), i.e., the probability of detecting n photon counts in a certain time-window, $P(\theta|n)$ is the distribution of the sum of delay-time bin numbers, provided there are n photon counts from above (Eq. 15).

The combination of Eqs. 4, 8, 15, and 16 leads to the following expression. (According to Eq. 17, each column of the $G(\xi, \eta)$ matrix corresponding to a given value is a one-dimensional Fourier transform of the function $P^{FIDA}(n)[G^{FLA}(\eta)]^{n}$, whereas, according to Eq. 18, each element of the $G(\xi, \eta)$ matrix can also be expressed as a Fourier image of $P^{FIDA}(n)$ at the point $\xi G^{FLA}(\eta)$.)

$$G(\xi, \eta) = \sum_{n} P^{FIDA}(n)[G^{FLA}(\eta)]^{n}\xi^{n} \quad (17)$$

$$= G^{FIDA}(\xi G^{FLA}(\eta)), \quad (18)$$

which, in combination with Eqs. 9 and 18, leads to the generating function $G(\xi, \eta)$ of $P(n, \theta)$,

$$G(\xi, \eta) = \exp\left[c \int dV(\exp\{[\xi G^{FLA}(\eta) - 1]qB(\mathbf{r})T\} - 1)\right]. \quad (19)$$

So far, we have only derived a theoretical expression for the case of a single species. However, because of assumption 1 fluorescence contributions from different species or background contributions can be easily accounted for by convoluting the single-species expressions or by the product of their generating functions.

Concerning background contributions, we have to distinguish between scattered and dark counts. Whereas the scattered component is directly related to the excitation pulses, dark counts of the detector have a fully random detection time and are hence not related to the excitation pulses. The two types of background count rates can be considered as two additional species, with mean count rates λ_{scat} and λ_{dark}, which are both Poissonian in nature. Whereas the distribution of scatter counts, $P_{IRF}^{FLA}(k)$, is given by the IRF, the distribution of delay times of dark counts, $P_{dark}^{FLA}(k)$, does not vary over the delay time bins of a pulse period, and may consequently be assumed constant. With respect to FIDA, they both contribute with a factor of the form $\exp[(\xi - 1)\lambda T]$ to the generating function, $G^{FIDA}(\xi)$, because the generating function of a Poisson distribution with the mean, λT, is $\exp[(\xi - 1)\lambda T]$. In combination with Eq. 18, the respective FILDA expressions for the generating functions or Fourier images of the background components therefore read

$$G_{dark}(\xi, \eta) = \exp[(\xi G_{dark}^{FLA}(\eta) - 1)\lambda_{dark}T], \quad (20)$$

$$G_{scat}(\xi, \eta) = \exp[(\xi G_{IRF}^{FLA}(\eta) - 1)\lambda_{scat}T]. \quad (21)$$

At this point, we now have all pieces collected that are necessary to formulate a closed expression for the theoretical model function that can be fitted against the experimentally acquired data. For multiple species including both types of background counts, Eqs. 19 to 21 combined yield the final expression of the generating function,

$$G(\xi, \eta) = \exp[(\xi G_{dark}^{FLA}(\eta) - 1)\lambda_{dark}T + (\xi G_{IRF}^{FLA}(\eta) - 1)\lambda_{scat}T + \sum_{j} c_j \int dV(\exp\{[\xi G_j^{FLA}(\eta) - 1]q_j B(\mathbf{r})T\} - 1)], \quad (22)$$

where the subscript, j, denotes contributions from different species. The calculation of the 2D Fourier transform of Eq. 22 completes the calculation of the theoretical distribution function, $P(n, \theta)$ (cf. Eq. 4). Thus, by fitting the FILDA distribution calculated in this manner, the absolute concentration, c_j, specific brightness, q_j, and the fluorescence lifetime, τ_j, of the different fluorophores under observation can be determined from a single, one-detector experiment.

Fitting algorithms

Fitting to the experimental data is carried out by calculating theoretical distributions with varying parameters, c_j, q_j, and τ_j (and, in exceptional cases, also a_1, a_2, a_3, and λ_{dark} and λ_{scat}), and minimizing the deviations between theory and

experiment. In most photon histogramming techniques, the quantification of the deviations is usually carried out using one of two different methods, the maximum likelihood or least squares method (Baker and Cousins, 1984).

FILDA is by no means limited to any particular fitting algorithm. The functions we apply for fitting are of a rather general use, only the calculation of the theoretical distribution, $P(n, \theta)$, is specific. As the best fit criterion, one can either use a maximum likelihood or a least squares method, which, as derived in the Appendix, yields identical results provided the weights in the least squares method are appropriately selected. However, at this point, it is worth noting that the usefulness of the least squares method at low event numbers, as they frequently occur in FILDA experiments, is controversially discussed in the literature. Hall and Selinger (1981), Köllner and Wolfrum (1992), and Maus et al. (2001) affirm that only maximum likelihood methods can be used, whereas least squares methods always yield biased estimates. We think that the reason for these deviations is the use of experimental weights in connection with the least squares method.

Because the theoretical FILDA model $P(n, \theta)$ is not linear with respect to the parameters, fitting is inevitable iterative in nature. We have used Marquardt algorithm for fitting with weights as outlined below, both in the case of the least squares and the maximum likelihood method. Typically, the mathematical problem converges in 5–15 iterations.

Weights

For simplification, we assume that count numbers in consecutive counting time intervals are independent. Although this assumption is not strictly correct, because molecular coordinates may be correlated over a few counting time intervals, it has already been successfully used in FIDA. Under this assumption, the number of events with a given pair, (n, θ), is binomially distributed around the mean, $MP(n, \theta)$, where M is the number of counting time intervals per experiment. This yields the following expression for weights, $W(n, \theta)$, of the least squares problem

$$\chi^2 = \sum_{n,\theta} W(n, \theta)[\hat{P}(n, \theta) - P(n, \theta)]^2 = \min,$$

$$W(n, \theta) = \frac{M}{P(n, \theta)}, \qquad (23)$$

where $\hat{P}(n, \theta)$ is the measured FILDA histogram, and $P(n, \theta)$ is the theoretical distribution.

Calculation of theoretical FLA distributions

Along with FILDA, we have also applied ordinary FLA in this study for comparative purposes. Here, we shall therefore describe how the theoretical FLA distribution has been calculated. The fit curve for FLA has been addressed in detail in other publications (Grinvald and Steinberg, 1974; Lakowicz, 1983; Zander et al., 1996). However, the basic procedure that describes a simple theoretical excitation-to-detection delay-time histogram was given in Eqs. 11 and 12. In the case of a measurement involving multiple species, j, with different fluorescence lifetimes, τ_j, an appropriate weighting of the different contributions must be ensured. This is necessary because the different species contribute to the decay histogram according to their fractional fluorescence count rates, λ_j. The fractional count rates, in turn, are given by the product of the individual molecular concentration, c_j, and their specific brightness values, q_j, ($\lambda_j = c_j q_j$). In the theoretical fluorescence decay function, $P^{FLA}_{decay}(t)$, used for fitting throughout this paper, the fractional count rates, λ_j, are directly determined by introducing the mean total count rate, λ_{tot}, of the measurement. Furthermore, background terms due to scattered and dark counts are taken into account according to their distributions, $P^{FLA}_{IRF}(t)$ and $P^{FLA}_{dark}(t)$, with mean count rates, λ_{scat} and λ_{dark} (compare Eqs. 20 and 21). This yields the expression

$$\lambda_{tot} P^{FLA}_{decay}(t) = \left[P^{FLA}_{IRF}(t) \otimes \sum_j \lambda_j \frac{1}{\tau_j} \frac{1}{1 - e^{-T_{pulse}/\tau_j}} e^{-t/\tau_j} \right] + \lambda_{scat} P^{FLA}_{IRF}(t) + \lambda_{dark} P^{FLA}_{dark}(t), \qquad (24)$$

whereas convolution with the (normalized) IRF and transformation to the bin number axis, k, is performed according to Eqs. 11 and 13 to fit the experimental excitation-to-detection delay time histogram, which is normalized to λ_{tot}.

Consequently, FLA, as performed throughout this paper, does not allow a direct determination of the absolute concentrations, c_j, and specific brightness values, q_j, but only their products, $\lambda_j = c_j q_j$. However, many FLA approaches use a slightly different expression with amplitudes, $A_j = \lambda_j/\tau_j$. These amplitudes are lifetime corrected and scale with the individual concentrations, c_j, if the lifetime, τ_j, is directly proportional to the specific brightness, q_j.

MATERIALS AND METHODS

Experimental equipment

A standard epi-illuminated confocal microscope (Evotec OAI, Hamburg, Germany) as used in fluorescence correlation spectroscopy (Koppel et al., 1976; Rigler et al., 1993) is the central optical component of a FILDA experiment. Because FILDA combines both continuous molecular brightness and time-resolved fluorescence lifetime analysis, a fast-pulsed laser diode (PDL 800, 635 nm, 6 mW, PicoQuant GmbH, Berlin, Germany) is used for excitation. With a repetition rate of 80 MHz, it may be considered as a quasi-continuous wave for the purposes of intensity fluctuation detection, whereas the resulting pulse interval of 12.5 ns and pulse width of 0.3 ns allows for a sufficiently precise examination of the fluorescence lifetime of the probes used.

For the excitation of fluorescence, the laser light passes a beam expander and is directed to the microscope objective (UApo/340, 40×, N.A. 1.15, Olympus Optical Co., Ltd., Tokyo, Japan) by a dichroic mirror (635LP, Chroma, Brattleboro, VT). Fluorescence is collected by the same

objective through the dichroic mirror, a spectral bandpass filter (670DF40, Omega, Brattleboro, VT), and is focused to a confocal pinhole, which serves to reject out-of-focus light. The light that passes the 70-μm pinhole, is detected by a silicon photon-counting avalanche diode (SPCM-AQ-131, EG&G Optoelectronics, Vaudreuil, Quebec, Canada).

Detector pulses and laser trigger pulses are passed to a computer plug-in card. This card, constructed at Evotec OAI, consists of two subunits, one of which is a time-correlated single-photon counting module. This module detects the delay time of a photon count with respect to the incident laser pulse. A time-to-digital converter quantifies this time information with bin width of $\Delta = 131$ ps and a conversion rate of up to 20 MHz. The typical bin-width value selected in FILDA is slightly higher than that used for FLA (0.524 vs. 0.131 ns) to circumvent excessive values of the integrated bin number, θ, and to minimize the number of data points to be fitted. Usually, the time-to-digital conversion is not distortion free because of electronic imperfections. Thus, the quality of analysis is improved by accounting for the individual width value of each bin, $\Delta_k = t_{k+1} - t_k$, as determined from a FLA histogram recorded at constant illumination.

The other subunit of the plug-in card is an electronic counter using an internal clock with a time resolution of 50 ns to obtain the time lag between any pair of successively detected photon counts (photon interval time). Thus, two independent times are simultaneously recorded for each photon count detected; the microscopic delay time (nanoseconds) of the photon counts with respect to the corresponding laser pulses containing the fluorescence lifetime information, and the macroscopic photon interval time (micro- to milliseconds) encoding the fluorescence intensity and fluctuation information. The 2D FILDA histogram is constructed from both the photon count numbers detected in a counting time interval of 100 μs and the sum of delay times collected during the same counting time interval. Furthermore, the one-dimensional FIDA histogram (100-μs counting time interval) and the FLA delay time distribution are calculated from the fluorescence raw data.

From FCS measurements, the mean diffusion times of the fluorescent dyes MR121, EVOblue™ 30 and Bodipy 630/650 were determined to be 200 μs. With a diffusion constant of $D = 3 \times 10^{-6}$ cm^2/s, this yields a radial $1/e^2$-radius of the detection volume of 0.5 μm (Rigler et al., 1993). The time-averaged laser beam power at the sample was 200 μW.

Experimental procedures

To characterize the equipment, four different calibration measurements were performed: with constant daylight illumination as a random source of photons to correct data for uneven channel width of the time-to-digital converter as outlined in the previous section; scattered light of the incident laser from a pure solvent sample to determine the IRF of the equipment; pure dye solution to determine the spatial brightness parameters of Eq. 10; and a measurement on pure water and with the excitation laser switched off to obtain independent estimates of the scattered Raman and dark count rates, λ_{scat} and λ_{dark}, respectively.

As an example, Fig. 2, *A* and *B*, show two different representations of the obtained FILDA histogram of an ~1-nM Bodipy 630/650 solution. The axes of abscissas represent the sum of delay times, θ, and the photon count numbers, n, as described above. Data for this histogram were collected for 2 s. Fitting this 2D histogram to the double Fourier transform of Eq. 22 yields the concentration or mean number of molecules in the detection volume, $c = 2.3$, the molecular brightness, $q = 23.2$ kHz, and the fluorescence lifetime, $\tau = 3.3$ ns. These values are in full agreement with the values determined by FIDA and FLA (data not shown) and with previously reported lifetimes for Bodipy 630/650 (Sauer et al., 1998). To judge the accuracy of the fit, a least square value of $\chi^2 = 1.1$ was calculated according to Eq. 23. As a comparison, Fig. 2 *C* shows the obtained FILDA histogram of a mixture of Cyanine 5 (approximately 0.5 nM) and Bodipy 630/650 (~0.2 nM) recorded in the same way. A two-component fit to the data results in values of $c_1 = 0.72$, $q_1 = 19.5$ kHz, $\tau_1 = 0.61$ ns and $c_2 = 0.27$, $q_2 = 23.3$ kHz, $\tau_2 = 3.1$ ns, and $\chi^2 = 1.2$. Both species can obviously

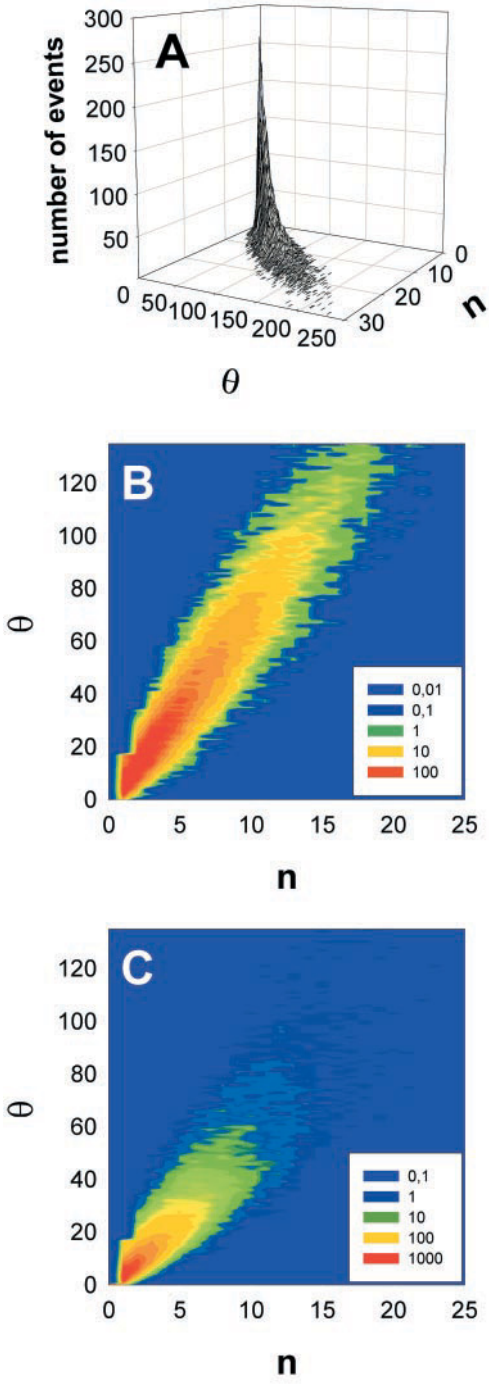

FIGURE 2 (*A*) (*B*) Two equivalent representations of a FILDA histogram from a Bodipy 630/650 solution (~1 nM). (*C*) FILDA histogram of a mixture of Cyanine 5 (~0.5 nM) and Bodipy 630/650 (~0.2 nM). In both cases, the data collection time was $T_C = 2$ s. The number of events plotted are (z-axis in (*A*) and colored in (*B*) and (*C*)) where a specific number of photon counts, n, with an integrated delay time, θ, has been detected during the counting time interval, $T = 100$ μs. The fit of Eq. 22 to the FILDA histogram resulted in values of (*A*) and (*B*) $c = 2.3$, $q = 23.2$ kHz, $\tau = 3.3$ ns, $a_1 = -0.41$, $a_2 = 0.09$, $a_3 = 1.0$ (fixed), and $\chi^2 = 1.1$, and (*C*) $c_1 = 0.72$, $q_1 = 19.5$ kHz, $\tau_1 = 0.61$ ns and $c_2 = 0.27$, $q_2 = 23.3$ kHz, $\tau_2 = 3.1$ ns, and $\chi^2 = 1.2$ (adjustment parameters fixed to the values of (*A*) and (*B*)). The background count rates $\lambda_{scat} = 0.4$ kHz and $\lambda_{dark} = 0.15$ kHz were predetermined from adjustment samples (water as solvent alone and laser switched off, respectively).

already be distinguished through the perturbation they cause to the shape of the FILDA distribution when compared with Fig. 2 *B*.

Data simulations

Samples composed of a mixture of molecules, which express deliberately chosen parameters (brightness and fluorescence lifetime values), are difficult to prepare. Therefore, certain evaluations were performed using simulated data. A number of histogram sets for FILDA, FIDA, and FLA were simulated according to the algorithm described in detail elsewhere (Palo et al., 2000). This algorithm includes a random walk of individual molecules and a conversion of brightness integrals into random count numbers. As a modification of this algorithm, a random detection delay time, depending on the lifetime of the given species, was additionally assigned to each photon, and the IRF used in simulations was selected to be identical to that of the real experiment. The random count numbers and delay times obtained were subsequently used to calculate histograms for FILDA, FIDA, and FLA.

We consider the simulations to be an adequate tool for estimating statistical errors of the extracted parameters. For this purpose, typically $N = 100$ realizations of experiments with a given set of molecular parameters were simulated.

The calmodulin–peptide interaction

Calmodulin (molecular weight 16.7) is a regulatory protein involved in a variety of Ca^{2+}-dependent cellular signaling pathways (Klee, 1988). Structures at atomic resolution have identified two similar domains with two Ca^{2+} binding sites each (Babu et al., 1985, 1988; Chattopadhyaya et al., 1992; Wilmann et al., 2000), which, for calmodulin in solution, are connected by a flexible linker (Ikura et al., 1992). Upon binding of Ca^{2+}, those residues that create the binding site for most target proteins become exposed to the solvent. The relevant peptide sequence from one of the target proteins (e.g., smooth muscle myosin light chain kinase [sm-MLCK]) KRRWKKNFIA, was chosen as the target peptide. At the C-terminus, an additional Lysine was introduced to label the C-terminus with a dye (MR121). Because the predominant interaction sites of the target peptide (which interacts with both calmodulin domains) have been identified as the C- and the N-terminus (Meador et al., 1992, 1993), the molecular environment of the dye should change upon binding. Fluorescence lifetime, molecular intensity, and FILDA data should therefore indicate a binding event.

Calmodulin was purchased from BIOMOL (Hamburg, Germany) (from bovine brain, Lot# P4639c, 1 mg, lyophilized). The protein was dissolved in 25 mM Tris/HCl pH 8 and stored in aliquots at 4°C. The peptide (H-KRRWKKNFIAK-NH_2) was synthesized at Evotec and labeled with MR121 (Abs. max. = 661 nm) at the C-terminal Lysine. The buffer used throughout all experiments included 25 mM Tris/HCl pH 8, 1 mM $CaCl_2$, 100 mM KCl, and 0.05% Pluronic. Calmodulin and the fluorescently labeled peptide were incubated for 10 min at room temperature before measurement.

Fluorescent dyes and probe handling

The dyes used in this study were Bodipy 630/650 (Molecular Probes, Eugene, OR), Cyanine 5 (Cy5) (Amersham Pharmacia Biotech, Uppsala, Sweden), MR 121 (Roche Diagnostics, Penzberg, Germany), and EVOblue™ 30 (Evotec OAI), which all have their excitation maximum at ~635 nm. Dye solutions were prepared in ultrapure water.

As samples, the fluorescent probes were prepared at concentrations ~1 nM. Because of adsorption of the molecules to glass surfaces, it is not adequate to determine their concentration values from dilution ratios; a much better estimate is given by FILDA and FIDA themselves because both methods yield the absolute concentrations of the fluorescence probes. All experiments were carried out at 22°C room temperature.

RESULTS AND DISCUSSION

A new method may be evaluated through comparison with known methods on the basis of statistical errors obtained from simulated data. Alternatively, the results of simple test experiments that utilize the same equipment and the same sequence of photon counts may be compared. An initial evaluation of FILDA was carried out by applying it to different dye solutions and mixtures and subsequently comparing the results with those from FLA and FIDA. One would expect that the different methods should yield nearly equal estimates of the common parameters whereas their statistical accuracy may differ significantly.

Test experiments and data simulation

Initially, a series of 40 measurements with duration of T_c = 2 s each were performed on single dye solutions of MR121 and EVOblue™ 30, and on a 2:1 dye mixture of EVOblue™ 30 and MR121 (total dye concentration 1 nM in each case). Data was acquired in parallel for FILDA, FIDA, and FLA. All data sets were fitted with a varying number of fixed parameters that were predetermined from experiments on the respective single-dye solutions. The estimated parameters for all three methods are summarized in Table 1. For the single-dye cases, FILDA was in no way statistically more accurate than a simple combination of FIDA and FLA. This is as expected because all the molecules in solution are identical, and there is no gain from grouping delay times in counting time windows according to bursts from individual molecules, as performed in FILDA.

In the case of the mixture of two dyes, the fits over all data sets resulted in different mean values and statistical errors of the numbers of molecules per species in the confocal volume, c_1 and c_2 (proportional to the concentration), their brightness values, q_1 and q_2, and their lifetimes, τ_1 and τ_2, depending on the method of analysis and the number of free parameters. In Table 1, these errors are denoted in parentheses in terms of the ratio of standard deviation to mean value (coefficient of variation, CV). Here we emphasize again, that FLA only directly reveals the fractional count rates, i.e., products c_1q_1 and c_2q_2, instead of c_1 and c_2 (cf. Eq. 14). If c_1 and c_2 are the only two parameters that are subject to fitting, i.e., both brightness and lifetime values are fixed to the predetermined values from the single dye measurements, FILDA and FLA are nearly equal in accuracy whereas FIDA shows higher CV values. The superiority of FILDA becomes apparent in the case where no a priori knowledge of the parameters is available. If there are four free parameters, e.g., when the two lifetime parameters are subject to fitting as well, the statistical errors of FILDA compared to FLA are notably reduced. This reduction is

TABLE 1 Parameters and their coefficients of variance as evaluated with FILDA, FLA, and FIDA

	Single Dyes						Dye Mixtures							
	MR121			EVOblue™ 30			2 free			4 free				6 free
	FILDA	FLA	FIDA	FILDA	FLA	FIDA	FILDA	FLA	FIDA	FILDA	FLA	FILDA	FIDA	FILDA
c_1	0.35	—	0.35	0.81	—	0.81	0.20	—	0.20	0.22	—	0.20	0.17	0.24
	(4.2)		(4.2)	(3.9)		(3.8)	(7.0)		(14.1)	(7.9)		(8.0)	(39.3)	(8.0)
c_2							0.48	—	0.47	0.44	—	0.49	0.50	0.44
							(4.6)		(10.3)	(6.5)		(5.6)	(13.6)	(6.4)
q_1/kHz	29.8	—	30.0	12.4	—	12.6	29.8	—	29.8	29.8	—	30.8	32.3	28.4
	(4.8)		(4.3)	(4.3)		(4.4)	(fix)		(fix)	(fix)		(5.5)	(14.4)	(5.4)
q_2/kHz							12.4	—	12.4	12.4	—	12.2	13.8	11.7
							(fix)		(fix)	(fix)		(4.9)	(13.1)	(5.3)
$(cq)_1$/kHz	—	10.1	—	—	10.0	—	—	5.99	—	—	6.89	—	—	—
		(4.7)			(3.0)			(7.5)			(8.3)			
$(cq)_2$/kHz							—	5.95	—	—	5.07	—	—	—
								(4.6)			(9.0)			
τ_1/ns	1.73	1.74	—	0.64	0.65	—	1.73	1.73	—	1.67	1.65	1.73	—	1.65
	(0.9)	(1.0)		(1.9)	(1.8)		(fix)	(fix)		(2.1)	(2.5)	(fix)		(1.7)
τ_2/ns							0.64	0.64	—	0.58	0.59	0.64	—	0.56
							(fix)	(fix)		(4.1)	(5.0)	(fix)		(4.1)

In all cases, 40 experiments with a data-acquisition time of 2 s each were performed on single-dye solutions of MR121 and EVOblue™ 30 (Single Dyes), and on a 1:2 dye mixture of MR121 and EVOblue™ 30 (Dye Mixture) with varying numbers of free parameters (named in the different columns). In the case of single dyes, all parameters are floating. Parameters that are fixed to values determined from the single dyes are denoted "fix", whereas the resulting CV values (coefficient of variation in percent, ratio of standard deviation to mean value of the results of the 40 experiments) of the freely fit parameters are given in parenthesis.

The parameters for each species, j, are the concentration c_j (mean number of particles in the detection volume) and brightness q_j for FIDA and FILDA, the fractional count rate as the product $(cq)_j$ for FLA, and the fluorescence lifetime τ_j for FLA and FILDA. The adjustment parameters $a_1 = -0.26$, $a_2 = 0.05$, and $a_3 = 1.0$ and background count rates $\lambda_{scat} = 0.4$ kHz and $\lambda_{dark} = 0.15$ kHz were predetermined from adjustment samples (1 nM aqueous MR121 solution, water as solvent alone, and laser switched off, respectively).

even better when the statistical errors are compared with those obtained from FIDA using free brightness values. Moreover, in the case of six fitted parameters, FILDA still gives convincing results with almost identical low CV values.

The strategy of fixing parameters to predetermined values can be applied to a number of biological assays monitoring, for instance, the binding of two molecules, one of which is fluorescent. In this case, one can indeed determine specific amounts of the free and bound state of the fluorescent compound in advance and fit only the two concentrations or fractional count rates. However, very often this scheme cannot be used, and a higher number of parameters must be fitted, in this case the use of FILDA becomes superior. Such cases may arise because multiple binding sites are involved and the specific brightness of the complex depends on the extent of binding and hence may not be fixed. Another example occurs in drug screening where the effects of certain chemical or natural compounds are tested with a biological target. The compounds are usually assumed to be nonfluorescent, but, in some cases, turn out to have autofluorescent properties. These samples may be fitted by inclusion of an additional species whose parameters characterize the autofluorescent compound, but which are not known beforehand.

From a practical point of view, the question arises as to whether FILDA remains highly accurate over a wide range of concentrations. Therefore, we simulated a series of 100 histograms for FILDA, FIDA, and FLA for different concentrations of a 1:1 mixture of two fluorescent species. We selected a twofold difference in the specific brightness ($q_1 = 30$ kHz and $q_2 = 15$ kHz) and in the lifetime ($\tau_1 = 3.0$ ns and $\tau_2 = 1.5$ ns) but an equal diffusion time (200 μs) for both species. All histograms were fitted to a two-component model with all parameters being subject to fitting. Because, at very low and at very high concentrations, all methods had difficulties in resolving the species unambiguously with a data acquisition time of $T_c = 2$ s, we prolonged this time to $T_c = 20$ s. Figure 3 shows the dependency of the statistical error of all three methods on the mean number of fluorescent dyes in the confocal volume, c_1 and c_2, which is proportional to and therefore denoted as the absolute concentration. The error is represented by the CV values of the concentration c_2 of the weakest signal ($q_2 = 15$ kHz). From Fig. 3, it is obvious that, within a concentration range of $c < 5$, FILDA reveals the lowest error but FLA is statistically more accurate only at significantly higher concentrations. This is not surprising because FLA solely depends on the number of detected photons, which scales linearly with the concentration. In contrast, FILDA and FIDA sense the relative fluctuations of the fluorescence signal which are reduced according to $\propto c^{-1/2}$. At extremely low concentrations, the fluores-

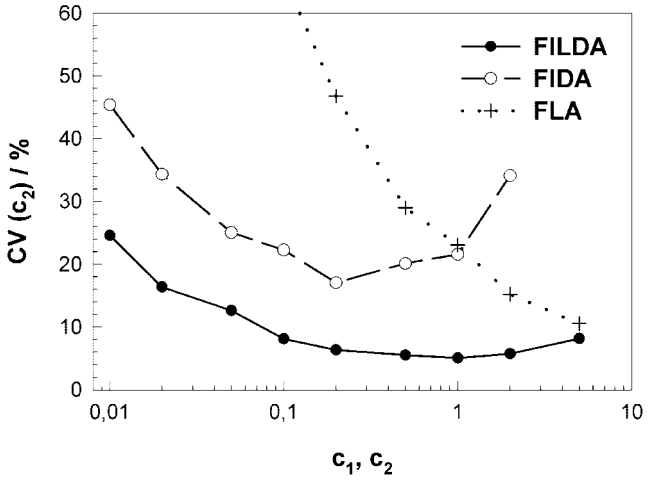

FIGURE 3 Dependency of the CVs of FILDA, FLA, and FIDA on the fluorescent species concentration, c_1 and c_2. The CV of the concentration value, c_2, of the second (*darker*) component is selected for representation on this graph. One hundred random histograms for each of the three methods were simulated for a 1:1 mixture of two fluorescent species at 20-s data collection time. The input parameters for the simulation were: concentration (mean number of particles in the detection volume) $c_1 = c_2$ (x-axis), brightness $q_1 = 30$ kHz and $q_2 = 15$ kHz, lifetime $\tau_1 = 3.0$ ns and $\tau_2 = 1.5$ ns. All parameters (c_1, c_2, q_1, q_2, τ_1, τ_2 in FILDA; c_1, c_2, q_1, q_2 in FIDA; and $(cq)_1$, $(cq)_2$, τ_1, τ_2 in FLA) were subject to fitting.

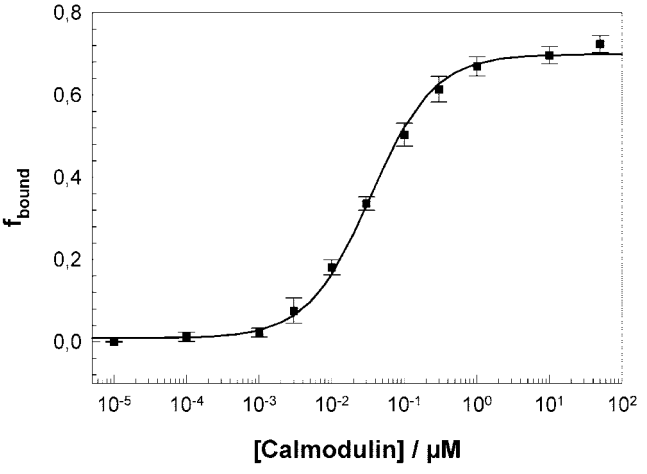

FIGURE 4 Binding of the labeled target peptide, H-KRRWKKNFIAK-NH_2, to calmodulin as monitored by FILDA (data collection time, $T_c = 2$ s, error bars from averaging over 10 repeated measurements). The solid curve results from a hyperbolic fit to the data, yielding a binding constant of $K_D = 34 \pm 3$ nM.

cence signal consists essentially of rare single-molecule events, which may possibly not be detected during a data collection time of 20 s. However, with a longer acquisition time, these rare events would more frequently be intercepted and are better approached using fluctuation methods such as FILDA and FIDA than with conventional FLA.

Biochemical System

The experimental utilization of FILDA was demonstrated by the determination of the binding constant of the calmodulin–peptide interaction mentioned above. For this purpose, a titration experiment was carried out, maintaining the labeled peptide (H-KRRWKKNFIAK-NH_2 (MR121)) concentration constant at 2.5 nM, while calmodulin was titrated (0, 0.01 nM, 0.1 nM, 1 nM, 3 nM, 10 nM, 30 nM, 0.1 μM, 0.3 μM, 1 μM, 10 μM, 50 μM). All experiments were performed under identical conditions, i.e., the same buffer, the same excitation power, and the same data acquisition time of 2 s per measurement, repeated 10 times per sample.

First, the adjustment parameters, $a_1 = -0.69$, $a_2 = 0.17$, and $a_3 = 1.0$, and background count rates, $\lambda_{scat} = 0.4$ kHz and $\lambda_{dark} = 0.15$ kHz, were obtained from adjustment samples (1 nM aqueous MR121 solution, water as solvent alone, and laser switched off, respectively) and fixed throughout further analysis. Afterwards, the lifetime, $\tau_{free} = 1.90 \pm 0.02$ ns, and the molecular brightness, $q_{free} = 6.5 \pm 0.3$ kHz, of the free peptide were determined from a single component analysis applied to the peptide solution alone. Addition of excess calmodulin (50 μM) to 2.5 nM peptide resulted in a sample with 74 $\pm$ 9% of the peptide bound to calmodulin under these assay conditions, as revealed from a two-component fit with fixed parameters for the free peptide. The complex was characterized both by a longer fluorescence lifetime, $\tau_{bound} = 3.29 \pm 0.13$ ns, and a higher molecular brightness, $q_{bound} = 16.7 \pm 0.8$ kHz, as compared to the free peptide.

In the next step, a similar two-component analysis was applied to the whole series of calmodulin concentrations. In these studies, the lifetime and brightness parameters were fixed to the above values for the bound and the free peptide. In this way, FILDA determines the concentrations of the bound peptide, c_{bound}, i.e., the calmodulin–peptide complex, and of the unbound, c_{free}, i.e., free peptide. This allows the calculation of the fraction of bound peptide, $f_{bound} = c_{bound}/(c_{bound} + c_{free})$, which is plotted against the concentration of added calmodulin in Fig. 4. The solid line shows a hyperbolic fit to the data, yielding a binding constant for the calmodulin–peptide interaction of $K_D = 34 \pm 3$ nM. Comparable binding curves were obtained by FLA and FIDA (data not shown) with similar K_D values of 16 $\pm$ 1 nM and 28 $\pm$ 4 nM, respectively. Again, it is noteworthy that, in the case of FLA, the bound fraction can only be estimated from the fractional count rates, i.e., the product cq that only reveals overall intensity ratios rather than absolute concentrations. Correcting these amplitudes for the known brightness values from FILDA, q_{bound} and q_{free}, results in a binding constant of $K_D = 38 \pm 3$ nM.

However, the K_D values are in good agreement with literature values reported for affinities (Barth et al., 1998), which demonstrates that FILDA, and the already

well accomplished methods FLA and FIDA, is a suitable method for monitoring the molecular interactions of a biochemical system. Furthermore, the outstanding statistical accuracy of FILDA combined with its fast data acquisition and processing makes it well suited for high-throughput screening purposes. To evaluate this area of application, we calculated the Z' factor from samples with high and low binding degrees (Zhang et al., 1999). The usage of this factor is widespread in the screening community because it reflects both the assay signal dynamic range and the data variation associated with the signal measurements. The Z' factor is a dimensionless, simple statistical characteristic defined as

$$Z' = 1 - \frac{3 \cdot [\sigma(f_{\text{high}}) + \sigma(f_{\text{low}})]}{f_{\text{high}} - f_{\text{low}}}, \tag{24}$$

with f_{high} and f_{low} being, in our case, the fraction bound under high (50 μM calmodulin) and low (pure peptide) binding conditions as determined from a two-component analysis, whereas $\sigma(f_{\text{high}})$ and $\sigma(f_{\text{low}})$ represent their respective standard deviations. The factor's maximum value is a Z' value of 1.0, and any screening application is counted for being robust and of high quality if $Z' > 0.5$ (Zhang et al., 1999).

For the calmodulin–peptide interaction (Fig. 4), we obtain, even for data acquisition times of only 2 s, a very high Z' factor of $Z' = 0.89 \pm 0.03$. This illustrates the suitability of FILDA for drug screening. To investigate the potential for further data-acquisition time reductions, as required for high-throughput applications, we determined the Z' factors for various data collection times T_c: Z' (T_c = 1 s) = 0.78 ± 0.06, Z' (T_c = 0.5 s) = 0.74 ± 0.07, Z' (T_c = 0.25 s) = 0.63 ± 0.09, and Z' (T_c = 0.1 s) = 0.36 ± 0.16. From this series, it is obvious that FILDA does indeed fulfill the prerequisites for efficient drug screening even at read out times below 1 s.

CONCLUSIONS

With FILDA, we have introduced another analysis method that is based on monitoring of fluctuations in the fluorescence signal from highly dilute samples and that is capable of distinguishing and quantifying species of a sample with different fluorescence properties. We have shown that FILDA can improve the accuracy of determining sample properties significantly, especially in the case of a high number of unknown fluorescence parameters beforehand. When compared with the well-established methods of FIDA and FLA, this is achieved by an increased number of two fluorescence parameters used to characterize each species. Especially, starting from FIDA, the implementation of the highly accurate but also very sensitive fluorescence lifetime parameter improves the accuracy of analysis immensely. Improvements in the fluorescence lifetime analysis are also achieved, because FILDA utilizes the fluorescence fluctuations and groups the excitation-to-detection delay times, which are necessary for lifetime determination, in counting time intervals according to bursts from individual molecules. However, this limits FILDA to a concentration range close to the single-molecule level, i.e., below several nanomolar. Nevertheless, these features make FILDA very attractive for various applications in life sciences, especially in the field of assay development and high-throughput drug screening.

APPENDIX: THE EQUIVALENCE OF THE MAXIMUM LIKELIHOOD AND THE LEAST SQUARES METHOD

In the following, we show that the maximum likelihood method leads to the same statistical estimates of parameters as the least squares method, provided the weights used remain constant even when the estimated parameters are varied. The notation used is the same as before, i.e., M is the number of counting time intervals, $\hat{\mathrm{P}}(n, \theta)$ is the measured FILDA histogram, and $\mathrm{P}(n, \theta)$ is the theoretical distribution. When fitting a theoretical model to the experimental data, the goal is to find an expression that can be minimized yielding the best set of estimated parameters, α.

Applying a maximum likelihood method means minimizing the expression,

$$L = -2 \sum_{\mathrm{n},\theta} M\hat{P}(n, \theta)\ln(\mathrm{P}(n, \theta)). \tag{A1}$$

Because

$$\sum_{\mathrm{n},\theta} \hat{P}(n, \theta) = \sum_{\mathrm{n},\theta} \mathrm{P}(n, \theta) = 1, \tag{A2}$$

we can add a zero-value term to Eq. A1, yielding

$$L = -2 \sum_{\mathrm{n},\theta} M(\hat{P}(n, \theta) - \mathrm{P}(n, \theta)) + M\hat{P}(n, \theta)\ln(\mathrm{P}(n, \theta)). \tag{A3}$$

In contrast, using a least squares method means minimizing

$$\chi^2 = \sum_{\mathrm{n},\theta} \frac{M}{\mathrm{P}(n, \theta)} (\hat{P}(n, \theta) - \mathrm{P}(n, \theta))^2, \tag{A4}$$

provided that the weights are taken from the optimal theoretical distribution. However, because, in our case, these weights are not known, the best we can do is to use constant weights during a single iteration step, i.e.,

$$\frac{\partial}{\partial \alpha} \frac{M}{\mathrm{P}(n, \theta)} = 0.$$

If we compare the derivatives with respect to the estimated parameters, α, of the two methods, we get from Eq. A3

$$\frac{\partial L}{\partial \alpha} = -2 \sum_{n,\theta} - M \frac{\partial \mathrm{P}(n,\theta)}{\partial \alpha} + M\hat{P}(n,\theta) \frac{\partial \mathrm{P}(n,\theta)}{\partial \alpha} \frac{1}{\mathrm{P}(n,\theta)} = -2 \sum_{n,\theta} \frac{M}{\mathrm{P}(n,\theta)} (\hat{P}(n,\theta) - \mathrm{P}(n,\theta)) \frac{\partial \mathrm{P}(n,\theta)}{\partial \alpha}, \tag{A5}$$

and, because the weights in Eq. A4 are kept constant,

$$\frac{\partial \chi^2}{\partial \alpha} = -2 \sum_{n,\theta} \frac{M}{\mathrm{P}(n,\theta)} (\hat{P}(n,\theta) - \mathrm{P}(n,\theta)) \frac{\partial \mathrm{P}(n,\theta)}{\partial \alpha}. \tag{A6}$$

It is obvious that, under these conditions, both expressions are equal and thus result in the same set of minimum values, i.e., the same set of estimated parameters, α.

The authors thank Drs. Ülo Mets and Vello Loorits for valuable contributions and Drs. Mary Cole and Nicholas Hunt for critically reading the manuscript. Mrs. Sonja Dröge is acknowledged for excellent assistance.

REFERENCES

Babu, Y. S., C. E. Bugg, and W. J. Cook. 1988. Structure of calmodulin refined at 2.2 Å resolution. *J. Mol. Biol.* 204:191–204.

Babu, Y. S., J. S. Sack, T. J. Greenhough, C. E. Bugg, A. R. Means, and W. J. Cook. 1985. Three-dimensional structure of calmodulin. *Nature.* 315:37–40.

Bajzer, Z., T. M. Therneau, J. C. Sharp, and F. G. Prendergast. 1991. Maximum likelihood method for the analysis of time-resolved fluorescence decay curves. *Eur. Biophys. J.* 20:247–262.

Baker, S., and R. D. Cousins. 1984. Clarification of the use of chi-square and likelihood functions in fits to histograms. *Nuclear Instrum. Methods Phys. Res.* 221:437–442.

Barth, A., S. R. Martin, and P. M. Bayley. 1998. Specificity and symmetry in the interaction of calmodulin domains with the skeletal muscle myosin light chain kinase target sequence. *J. Biol. Chem.* 273:2174–2183.

Brand, L., C. Eggeling, C. Zander, K. H. Drexhage, and C. A. M. Seidel. 1997. Single-molecule identification of coumarin-120 by time-resolved fluorescence detection—comparison of one- and two-photon excitation in solution. *J. Phys. Chem.* 101:4313–4321.

Brigham, E. O. 1974. The Fast Fourier Transform. Prentice-Hall, Englewood Cliffs, NJ.

Bunfield, D. H., and L. M. Davis. 1998. Monte Carlo simulation of a single-molecule detection experiment. *Appl. Opt.* 37:2315–2326.

Chattopadhyaya, R., W. E. Meador, A. R. Means, and F. A. Quiocho. 1992. Calmodulin structure refined at 1.7 A resolution. *J. Mol. Biol.* 228: 1177–1192.

Chen, Y., J. D. Müller, P. T. So, and E. Gratton. 1999. The photon counting histogram in fluorescence fluctuation spectroscopy. *Biophys. J.* 77: 553–567.

Clegg, R. M., and P. C. Schneider. 1996. Fluorescence lifetime-resolved imaging microscopy: a general description of lifetime-resolved imaging measurements. *In* Fluorescence Microscopy and Fluorescent Probes. J. Slavik, editor. Plenum Press, New York. 15–33.

Eggeling, C., S. Berger, L. Brand, J. R. Fries, J. Schaffer, A. Volkmer, and C. A. Seidel. 2001. Data registration and selective single-molecule analysis using multi-parameter fluorescence detection. *J. Biotechnol.* 86:163–180.

Elson, E. L., and D. Magde. 1974. Fluorescence correlation spectroscopy. I. Conceptual basis and theory. *Biopolymers.* 13:1–27.

Enderlein, J., P. M. Goodwin, A. van Orden, and W. P. Ambrose. 1997. A maximum likelihood estimator to distinguish single molecules by their fluorescence decay. *Chem. Phys. Lett.* 270:464–4706.

Fries, J. R., L. Brand, C. Eggeling, M. Köllner, and C. A. M. Seidel. 1998. Quantitative identification of different single molecules by selective time-resolved confocal fluorescence spectroscopy. *J. Phys. Chem.* 102: 6601–6613.

Grinvald, A., and I. Z. Steinberg. 1974. On the analysis of fluorescence decay kinetics by the method of least-squares. *Anal. Biochem.* 59: 583–598.

Hall, P., and B. Selinger. 1981. Better estimates of exponential decay parameters. *J. Phys. Chem.* 85:2941–2946.

Herten, D. P., P. Tinnefeld, and M. Sauer. 2000. Identification of single fluorescently labelled mononucleotide molecules in solution by spectrally resolved time-correlated single-photon counting. *Appl. Phys. B.* 71:765–771.

Ikura, M., G. Barbato, C. B. Klee, and A. Bax. 1992. Solution structure of calmodulin and its complex with a myosin light chain kinase fragment. *Cell Calcium.* 13:391–400.

Kask, P., K. Palo, N. Fay, L. Brand, Ü. Mets, D. Ullmann, J. Jungmann, J. Pschorr, and K. Gall. 2000. Two-dimensional fluorescence intensity distribution analysis: theory and applications. *Biophys. J.* 78:1703–1713.

Kask, P., K. Palo, D. Ullmann, and K. Gall. 1999. Fluorescence-intensity distribution analysis and its application in biomolecular detection technology. *Proc. Natl. Acad. Sci. U.S.A.* 96:13756–13761.

Kask, P., P. Piksarv, M. Pooga, Ü. Mets, and E. Lippmaa. 1989. Separation of the rotational contribution in fluorescence correlation experiments. *Biophys. J.* 55:213–220.

Keller, R. A., W. P. Ambrose, P. M. Goodwin, J. H. Jett, J. C. Martin, and M. Wu. 1996. Single-molecule fluorescence analysis in solutions. *Appl. Spectrosc.* 50:12A–32A.

Klee, C. B. 1988. Ca^{2+}-dependent phospholipid- (and membrane-) binding proteins. *Biochemistry.* 27:6645–6653.

Koppel, D. E., D. Axelrod, J. Schlessinger, E. L. Elson, and W. W. Webb. 1976. Dynamics of fluorescence marker concentration as a probe of mobility. *Biophys. J.* 16:1315–1329.

Köllner, M., and J. Wolfrum. 1992. How many photons are necessary for fluorescence-lifetime measurements? *Chem. Phys. Lett.* 200:199–204.

Lakowicz, J. R. 1983. Principles of Fluorescence Spectroscopy. Plenum Press, New York, London.

Magde, D., E. L. Elson, and W. W. Webb. 1972. Thermodynamic fluctuations in a reacting system-measurement by fluorescence correlation spectroscopy. *Phys. Rev. Lett.* 29:704–708.

Maus, M., M. Cotlet, J. Hofkens, T. Gensch, F. C. de Schryver, J. Schaffer, and C. A. Seidel. 2001. An experimental comparison of the maximum likelihood estimation and nonlinear least-squares fluorescence lifetime analysis of single molecules. *Anal. Chem.* 73:2078–2086.

Meador, W. E., A. R. Means, and F. A. Quiocho. 1992. Target enzyme recognition by calmodulin: 2.4 Å structure of a calmodulin-peptide complex. *Science.* 257:1251–1255.

Meador, W. E., A. R. Means, and F. A. Quiocho. 1993. Modulation of calmodulin plasticity in molecular recognition on the basis of x-ray structures. *Science.* 262:1718–1721.

Muller, R., C. Zander, M. Sauer, M. Deimel, D. S. Ko, S. Siebert, J. Ardenjacob, G. Deltau, N. J. Marx, K. H. Drexhage, and J. Wolfrum. 1996. Time-resolved identification of single molecules in solution with a pulsed semiconducter diode laser. *Chem. Phys. Lett.* 262:716–722.

O'Connor, D. V., and D. Phillips. 1984. Time-Correlated Single Photon Counting. Academic Press, New York.

Palo, K., Ü. Mets, S. Jäger, P. Kask, and K. Gall. 2000. Fluorescence intensity multiple distributions analysis: concurrent determination of diffusion times and molecular brightness. *Biophys. J.* 79:2858–2866.

Prummer, M., C. G. Hubner, B. Sick, B. Hecht, A. Renn, and U. P. Wild. 2000. Single-molecule identification by spectrally and time resolved fluorescence detection. *Anal. Chem.* 72:443–447.

Rigler, R., Ü. Mets, J. Widengren, and P. Kask. 1993. Fluorescence correlation spectroscopy with high count rate and low background: analysis of translational diffusion. *Eur. Biophys. J.* 22:169–175.

Sauer, M., J. Ardenjacob, K. H. Drexhage, F. Gobel, U. Lieberwirth, K. Muhlegger, R. Muller, J. Wolfrum, and C. Zander. 1998. Time-resolved identification of individual mononucleotide molecules in aqueous solution with pulsed semiconductor lasers. *Bioimaging.* 6:14–24.

Schwille, P., F. J. Meyer-Almes, and R. Rigler. 1997. Dual-color fluorescence cross-correlation spectroscopy for multicomponent diffusional analysis in solution. *Biophys. J.* 72:1878–1886.

Stokes, G. G. 1852. On the change of refrangibility of light. *Phil. Trans. R. Soc. Lond.* 142:463–562.

Ullmann, D., M. Busch, and T. Mander. 1999. Fluorescence correlation spectroscopy-based screening technology. *Innovations Pharm. Technol*. 30–40.

van Orden, A., N. P. Machara, P. M. Goodwin, and R. A. Keller. 1998. Single-molecule identification in flowing sample streams by fluorescence burst size and intraburst fluorescence decay rate. *Anal. Chem.* 70:1444–1451.

Weber, G. 1981. Resolution of the fluorescence lifetimes in a heterogeneous system by phase and modulation measurements. *J. Phys. Chem.* 85:949–953.

Wild, U. P., A. R. Holzwarth, and H. P. Good. 1977. Measurement and analysis of fluorescence decay curves. *Rev. Sci. Instrum.* 48:1621–1627.

Wilmann, M., M. Gautel, and O. Mayans. 2000. Activation of calcium/calmodulin regulated kinases. *Cell Mol. Biol. (Noisy-le-grand).* 46: 883–894.

Xie, X. S., and J. K. Trautman. 1998. Optical studies of single molecules at room temperature. *Annu. Rev. Phys. Chem.* 49:441–480.

Zander, C., M. Sauer, K. H. Drexhage, D. S. Ko, A. Schulz, J. Wolfrum, L. Brand, C. Eggeling, and C. A. M. Seidel. 1996. Detection and characterization of single molecules in aqueous solution. *Appl. Phys.* 63:517–523.

Zhang, J. H., T. D. Chung, and K. R. Oldenburg. 1999. A simple statistical parameter for use in evaluation and validation of high throughput screening assays. *J. Biomol. Screen.* 4:67–73.